Motor terminal degeneration unaffected by activity changes in SOD1G93A mice; a possible role for glycolysis

Dario Carrasco, *Emory University*
Edyta K. Bichler, *Morehouse University*
Mark M. Rich, *Wright State University*
Xueyong Wang, *Wright State University*
Kevin L. Seburn, *The Jackson Laboratory*
Martin J. Pinter, *Emory University*

Journal Title: Neurobiology of Disease
Volume: Volume 48, Number 1
Publisher: Elsevier: 12 months | 2012-10, Pages 132-140
Type of Work: Article | Post-print: After Peer Review
Publisher DOI: 10.1016/j.nbd.2012.06.017
Permanent URL: http://pid.emory.edu/ark:/25593/fk3t7

Final published version: http://dx.doi.org/10.1016/j.nbd.2012.06.017

Copyright information:

Published in final edited form as:
Neurobiol Dis. 2012 October ; 48(1): 132–140. doi:10.1016/j.nbd.2012.06.017.

Motor terminal degeneration unaffected by activity changes in SOD1^{G93A} mice; a possible role for glycolysis

Dario I. Carrasco[a], **Edyta K. Bichler**[b], **Mark M. Rich**[c], **Xueyong Wang**[c], **Kevin L. Seburn**[d], and **Martin J. Pinter**[a]

[a]Department of Physiology, Emory University, Atlanta, GA 30322

[b]Department of Neurobiology, Morehouse University School of Medicine, Atlanta, GA 30310

[c]Department of Neuroscience, Cell Biology and Physiology, Wright State University, Dayton, OH, 45435

[d]The Jackson Laboratory, Bar Harbor, ME 04609

Abstract

This study examined whether activity is a contributing factor to motor terminal degeneration in mice that overexpress the G93A mutation of the SOD1 enzyme found in humans with inherited motor neuron disease. Previously, we showed that overload of muscles accomplished by synergist denervation accelerated motor terminal degeneration in dogs with hereditary canine spinal muscular atrophy (HCSMA). In the present study, we found that SOD1 plantaris muscles overloaded for 2 months showed no differences of neuromuscular junction innervation status when compared with normally loaded, contralateral plantaris muscles. Complete elimination of motor terminal activity using blockade of sciatic nerve conduction with tetrodotoxin cuffs for 1 month also produced no change of plantaris innervation status. To assess possible effects of activity on motor terminal function, we examined the synaptic properties of SOD1 soleus neuromuscular junctions at a time when significant denervation of close synergists had occurred as a result of natural disease progression. When examined in glucose media, SOD1 soleus synaptic properties were similar to wildtype. When glycolysis was inhibited and ATP production limited to mitochondria, however, blocking of evoked synaptic transmission occurred and a large increase in the frequency of spontaneous mEPCs was observed. Similar effects were observed at neuromuscular junctions in muscle from dogs with inherited motor neuron disease (HCSMA), although significant defects of synaptic transmission exist at these neuromuscular junctions when examined in glucose media, as reported previously. These results suggest that glycolysis compensates for mitochondrial dysfunction at motor terminals of SOD1 mice and HCSMA dogs. This compensatory mechanism may help to support resting and activity-related metabolism in the presence of dysfunctional mitochondria and prolong the survival of SOD1 motor terminals.

Corresponding author: Martin J. Pinter, Department of Physiology, Emory University School of Medicine, 615 Michael St., Atlanta, GA 30322, Voice: 404-727-3472, Fax: 404-727-2648, mpinter@emory.edu.

Keywords

motor neuron disease; neurodegeneration; motor terminal; HCSMA; SOD1; G93A; mitochondria; glycolysis

INTRODUCTION

In at least 2 animal models of motor neuron disease (SOD1 mice and hereditary canine spinal muscular atrophy or HCSMA), degeneration begins at the motor terminal in the periphery (Fischer et al., 2004; Rich et al., 2002a; Rich et al., 2002b). Thus motor unit function is lost not because of cell death but because neuromuscular synaptic function is lost. The reason for initial loss of motor terminals is unknown. One notable feature of normal motor terminals is a dense supply of mitochondria (Yoshikami and Okun, 1984). Accumulating evidence indicates that mitochondrial dysfunction is a component of the disease process in SOD1 mice (Damiano et al., 2006; Panov et al., 2012; Pedrini et al., 2010; Santa-Cruz et al., 2012), including evidence for dysfunction at the motor terminal (David et al., 2007; Nguyen et al., 2011). The dense supply of mitochondria at motor terminals likely reflects the relatively large metabolic demands of maintaining ionic equilibrium in a small structure featuring a high surface to volume ratio. In addition, motor terminals are subjected to frequent influxes of several ionic species (including Ca2+) that must be cleared rapidly to prepare for subsequent activity and to maintain ionic equilibrium. Although other cellular components contribute, mitochondria play a central role in these processes, both as a source of ATP and as a temporary storage site for cytoplasmic Ca2+ (Babcock and Hille, 1998; Garcia-Chacon et al., 2006; Nicholls and Fergusen, 2002). Thus, motor terminals may be particularly vulnerable to mitochondrial dysfunction, and reports that the mitochondrial transition pore may open during repetitive activity in SOD1 mouse motor terminals indicate that action potential activity itself could eventually become an important contributing factor to motor terminal degeneration (Nguyen et al., 2011).

Previously, we showed that increased motor neuron activity accelerated motor terminal degeneration in HCSMA (Carrasco et al., 2004). Although evidence of mitochondrial dysfunction was lacking for HCSMA, the contribution of activity to degeneration was consistent with the pattern of motor unit involvement in which normally more active, slow-type motor units became dysfunctional before fast-type motor units (Pinter et al., 1995). In the SOD1 model, where direct evidence for mitochondrial dysfunction at motor terminals exists (David et al., 2007; Nguyen et al., 2011), the pattern of motor unit involvement is not readily explained by a contribution of activity to motor terminal degeneration. Motor units containing type IIb muscle fibers become dysfunctional well before other types (Frey et al., 2000; Hegedus et al., 2007; Hegedus et al., 2008; Pun et al., 2006), but other evidence indicates that type IIb units are likely to be the least active of all motor units (Hennig and Lomo, 1985). Reports on effects of increased activity in SOD1 mice are inconsistent; moderate or regular exercise has been reported to be beneficial (Carreras et al., 2010; Kirkinezos et al., 2003; Veldink et al., 2003), increased neuromuscular activity is reported to prolong survival of motor units (Gordon et al., 2010) while others report that strenuous exercise accelerates disease progression (Mahoney et al., 2004).

The primary focus of this study was to determine whether activity plays a role in determining motor terminal degeneration in SOD1 mice. To accomplish this, muscles were overloaded using synergist denervation or paralyzed by conduction blockade of the sciatic nerve. The results showed that neither of these manipulations affected muscle innervation status. Recordings of endplate currents from muscles likely to experience increased activity late in the disease course showed that synaptic function was relatively normal under

standard conditions. However, when glycolysis was inhibited to test mitochondrial metabolic support, significant increases in the frequency of spontaneous endplate currents and some blocking of evoked endplate currents occurred at SOD1 endplates but not at wildtype endplates. Similar effects were observed in sampling from a limited number of HCSMA endplates. The results are considered in terms of mechanisms that may compensate for dysfunctional mitochondria at motor terminals.

METHODS

Animals

All transgenic mice used in this study derived from an inbred congenic strain of mice B6.Cg-Tg(SOD1-G93A)1Gur/J carrying the G93A mutant form of the human SOD1 transgene (Gurney et al., 1994). In this paper, these mice are referred to as B6.SOD1. These mice exhibit early changes in motor performance (ca. 50 days) but survive about 1 month longer than B6SJL SOD1 transgenic mice (Wooley et al., 2005). All mice were acquired from The Jackson Laboratory (www.jax.org, Bar Harbor, ME).

A total of 3 dogs were used in this study; 2 were obtained from the HCSMA breeding colony previously maintained at Emory University and showed motor symptoms typical of HCSMA homozygotes (Pinter et al., 2001). The other dog was purpose-bred and obtained from a commercial vendor to provide a genetically-normal control for data comparison. All experiments were carried out in accordance with the Institutional Animal Care and Use Committees of Emory University and the Jackson Laboratories.

Overload procedure

Mice were anesthetized with isoflurane (1.5–2%) and an incision was made in the dorsal aspect of the left leg at the level of the popliteal fossa to expose the sciatic nerve and the rostral portion of the triceps surae muscles. Nerve branches innervating the lateral gastrocnemius (LG), soleus and the medial gastrocnemius (MG) were located, exposed and freed. A ligature (6.0 silk) was passed around each nerve near the entry point to the muscle and then tightly ligated. The nerves were cut distal to the ligature and the cut ends of each nerve were freed to allow them to be deflected as far as possible from the denervated muscle to prevent reinnervation.

Following the overload period, prior to sacrifice and tissue harvesting, the mice were anesthetized and underwent surgery to confirm that reinnervation had not occurred. In all animals, ligated nerve endings were located and visually inspected using a dissecting microscope for evidence of reconnection to denervated muscles. In most animals, it could be visually confirmed that ligated nerve endings were not reconnected. In ~ 1/3 of the animals, where visual confirmation was uncertain, a stimulus was applied to the sciatic nerve while holding the exposed tendons of denervated muscles with forceps to confirm the absence of muscle force. Finally, plantaris (overloaded) as well as soleus, LG and MG (denervated) muscles were harvested bilaterally and weighed to further confirm the effectiveness of denervation/overload (See Results).

Blockade of sciatic conduction

Conduction blockade of the sciatic nerve was produced by continuous superfusion of tetrodotoxin (TTX) delivered by a system consisting of a mini-osmotic pump (Alzet, model 2002), a silastic cuff and a connecting tube (Silastic tubing, Dow Corning). Under general anesthesia, an incision was made at the popliteal fossa to expose the sciatic nerve and another small incision was made on the upper back. The sciatic nerve was separated from surrounding connective tissue and the cuff was gently placed around the nerve above the

level of the knee and closed with two loops of suture. The connecting tube was passed beneath the skin and led proximally through the back incision into the mid back region and connected to the osmotic pump. The pump and the silastic tube were filled with a solution containing TTX (150 μg/ml) and dexamethasone (3.7 μg/ml; Abraxis Pharmaceutical products). The pump was placed beneath the skin and anchored by suture to subcutaneous connective tissue. During the treatment period, successful nerve blockade was indirectly determined by the absence of ankle extension during walking. At the end of the TTX treatment period, complete paralysis was verified by total absence of contraction of hind limb muscles during electrical stimulation of the sciatic nerve proximal to the cuff. The stimulus intensity used was 2x the threshold value required to observe contraction of the hind limb muscles when the nerve was stimulated distal to the cuff. Mice were excluded from the study if ankle extension and/or muscle contraction were observed.

Immunolabeling

Plantaris muscles from B6.SOD1mice were recovered from each limb and placed into 4% paraformaldehyde for 1 hr. Muscles were washed in a 0.1 M phosphate buffered solution (PBS) and incubated at 4°C overnight in PBS containing 20% sucrose for cryoprotection. Sections (50 μm thickness) were obtained using a Cyrostat (Leica). Motor endplate acetylcholine receptors (AChRs) were labeled with rhodamine conjugated α-bungarotoxin (Molecular Probes). Axons and motor nerve terminals were labeled with a mouse monoclonal antibody against the phosphorylated heavy fragment of neurofilament protein (SMI31, 1:400, Sternberger Monoclonal). Labeling was visualized using fluorescein-conjugated secondary antibody (1:100, Jackson Immunoresearch Laboratories). Synaptic vesicles were labeled using a rabbit polyclonal antibody directed at synaptophysin (1:100, Santa Cruz Biotechnology) and visualized using an AMCA-conjugated secondary antibody (1:100, Jackson Immunoresearch Laboratories). Labeled NMJs were viewed using an upright microscope equipped for epifluorescence (Leica). Image analysis consisted of evaluating NMJ innervation status for the extent to which presynaptic labeling overlaid postsynaptic labeling for AChRs in superimposed images. Three categories of innervation status were used as described previously (Carrasco et al., 2010; Carrasco et al., 2004). Fibers were considered fully innervated if presynaptic labeling for synaptic vesicles completely covered the entire endplate area labeled for AChRs when images of vesicle and AChR labeling were superimposed. Fibers were considered partially innervated or denervated if only part or none, respectively, of the endplate labeled for ACh receptors area was occupied by the synaptic vesicles staining. For analysis, randomly selected fields of NMJs were first located at low magnification. All the NMJs in each field were then categorized as described above. Endplates were examined in 100–125 muscle fibers in each muscle.

Endplate recording

Endplate recordings were obtained from the soleus muscle of B6.SOD1 mice and from the MG muscle of HSCMA dogs. The soleus muscles of untreated B6.SOD1 and wildtype mice were dissected free and removed under general anesthesia (ketamine, 95 mg/kg; xylazine, 5 mg/kg). Samples from the MG muscle of dogs were obtained as described previously (Rich et al., 2002a). For both preparations, endplate recording was performed as previously described (Wang et al. 2004; Wang et al. 2006; Wang et al. 2010, Rich et al 2002). Briefly, after dissection, muscles were pinned in a sylgard-lined dish, stained with 10 M 4-(4-diethylaminostyryl)-N-methylpyridinium iodide (4-Di-2ASP; Invitrogen, Carlsbad, CA) and imaged with an upright epifluorescence microscope (Leica). **T**he recording chamber was continuously perfused with Ringer solution containing (in mM per liter) NaCl, 118: KCl, 3.5; $CaCl_2$, 2; $MgSO_4$, 0.7; $NaHCO_3$, 26.2; NaH_2PO_4, 1.7; glucose, 5.5 (pH 7.3–7.4, 20–22°C) equilibrated with 95% O_2 and 5% CO_2. Muscle fibers were crushed away from the endplate band to depolarize muscle fibers and eliminate contractions following nerve

stimulation. Two electrode voltage clamp recording was used, and muscle fibers were impaled within 100 μm of the endplate to ensure good space clamp of the endplate region. Holding potentials were set to −50 mV. In SOD1 soleus muscles, mEPCs were recorded for 1 min without stimulation, while periods of up to 4 mins were used to record mEPCs in dog MG muscle fibers. To obtain EPC records, nerves were stimulated with 0.2-ms current pulses at 0.5 Hz using a bipolar electrode (FHC, Bowdoin, ME). For all experiments, quantal content was calculated by dividing mean peak EPC current amplitude by mean peak mEPC current amplitude. All recording was performed at room temperature.

During some experiments, the standard bathing solution described above was replaced with a solution that contained 11 mM pyruvate instead of 5.5 mM glucose. This switch of bathing fluid was performed after records of EPCs and mEPCs from 7–11 muscle fibers were first obtained. After the switch, records were obtained from 7–10 additional but different muscle fibers. The purpose of this switch is to inhibit glycolysis by eliminating its substrate (glucose) but to continue providing exogenous pyruvate for oxidation by mitochondria. This manipulation is based on similar experiments on isolated synaptosomes (Kauppinen and Nicholls, 1986a; Kauppinen and Nicholls, 1986b) and is intended to functionally isolate ATP production to motor terminal mitochondria in order to test mitochondrial capacity to support motor terminal synaptic function. Further details are provided in the Results section.

Statistics

Statistical comparisons of innervation status data were made between the treated (left side, overload or TTX) and the contralateral control (right) plantaris muscles. For analysis, two-way contingency tables (innervation status vs. muscle source, treated or contralateral control) were used to determine whether statistically significant differences existed in the percentage of innervated and denervated endplates observed between treated and control plantaris muscles. To enable use of two-way tables, counts of partially innervated and denervated endplates were merged into one category characterized as being not fully innervated. The Mantel-Haenszel test for 2 × 2 contingency tables was used to test for association between innervation and muscle source in individual animals while controlling for possible effects of different animals. For continuous variables, split-plot analysis of variance was used to determine the significance of treatment effects and Tukey's honestly significant difference post-hoc test was to test the significance of differences between treatment groups. All analysis was performed using commercially available software (Systat Inc). Mean values are presented ± 1 SEM.

RESULTS

Overload of B6.SOD1 muscles

Studies have shown that surgical denervation of close synergists increases motor unit activity in muscles (Gardiner et al., 1986; Pearson et al., 1999). Previously, this approach was used to show that increased activity accelerated motor terminal degeneration in a canine version of motor neuron disease (HCSMA) (Carrasco et al., 2004). To determine whether this treatment accelerates motor terminal degeneration in SOD1 mice, we surgically denervated the left MG, LG and soleus muscles in B6.SOD1 mice aged 30–35 days, thus transferring the full load of ankle extension to the normally innervated plantaris muscle. An analysis of untreated plantaris muscles from B6.SOD1 mice aged about 70 days (N = 3) showed an average of 98% completely intact NMJ innervation. We thus infer that overload treatment began well before plantaris muscles normally begin to show motor terminal degeneration. Overload treatment continued for 60–65 days, or until mice were aged 90–100 days. At this age B6.SOD1 mice normally remain mobile. The purpose of this design was to insure that overload was present before the average onset of motor terminal degeneration so

that possible effects of increased activity on both the initiation and progression of motor terminal degeneration could be assessed. At the conclusion of overload treatment, plantaris, MG, LG and soleus muscles from both sides of each treated B6.SOD1 animal were recovered and weighed. In addition the innervation status of plantaris NMJs was analyzed. We found that the weights of overloaded plantaris muscles had increased about 35% on average relative to untreated contralateral plantaris muscles and that all denervated muscles had lost weight compared to innervated contralateral muscles by an average of about 40%. The increased plantaris weights fit with the results of previous studies in which overload increased force outputs of motor units in overloaded plantaris muscles in rat (Gardiner et al., 1986).

Analysis of plantaris NMJs showed that overload of the plantaris muscle produced no significant changes of average innervation status of muscle fibers relative to the contralateral, untreated muscle. Figure 1 shows the percentages of plantaris endplates in each of 3 innervation categories for all B6.SOD1 animals tested (N = 6) along with mean values for each category (solid symbols). In all cases, data tended to cluster around the identity line indicating that no differences existed between overloaded and contralateral, untreated muscles ($p > 0.05$, Mantel-Haenszel test). The similarity of innervation status in both overloaded and control plantaris muscles demonstrates that motor terminal degeneration proceeded at the same overall rates on both sides. These results show that overload of B6.SOD1 hindlimb muscles for a relative long period (2 months) has no effect on B6.SOD1 muscle innervation status.

TTX blockade of sciatic conduction in B6.SOD1 mice

One explanation for the lack of an overload effect on muscle innervation status is that the treatment did not increase activity in plantaris muscles sufficiently beyond that which the animals themselves normally produce. We thus decided to take an opposite approach and performed experiments in which motor terminal action potential activity was eliminated by conduction blockade of the sciatic nerve. At age 70 days, sciatic nerves of B6.SOD1 animals were fitted with silastic cuffs connected to osmotic pumps filled with a solution of tetrodotoxin (TTX). We selected this age so that TTX treatment would begin at about the same time that motor terminal degeneration commences in the plantaris muscle (about 70 days, see above). The specific question addressed in this experiment is thus whether motor terminal degeneration can be slowed after it begins by the complete absence of motor terminal action potential activity. TTX treatment continued for 1 month, or until age 100 days when the effects of overload treatment were also assessed. At this time, paralyzed and contralateral untreated plantaris muscles were recovered and compared for NMJ innervation status. Figure 2 shows that no differences of plantaris innervation status were observed between the treated and untreated sides ($p > 0.05$, Mantel-Haenszel test). These results show that the motor terminal degenerative process in B6.SOD1 mice progresses normally even in the absence of motor terminal action potential activity.

Comparison of Figure 1 and 2 shows that the levels of plantaris muscle denervation differed between the 2 groups of B6.SOD1 mice used for overload and TTX experiments. These differences are unlikely to be related to treatment effects since detection of effects is based on comparisons of data from treated muscles with data from paired, untreated, contralateral muscles, and these comparisons reveal no evidence of treatment effects. The differences between the data evident in Figs 1 and 2 likely reflect quantitative differences in disease expression among B6.SOD1 mice that can be seen elsewhere this study (see Figure 5B) and have been observed in previous studies (Carrasco et al., 2010).

B6.SOD1 soleus motor terminal physiology

A related question is whether activity promotes synaptic dysfunction prior to frank motor terminal degeneration in SOD1 mice, such as occurs in HCSMA (Balice-Gordon et al., 2000; Rich et al., 2002a). We first considered testing this idea using plantaris muscles from the overload experiments, but concluded that the extent of naturally occurring motor terminal degeneration that had occurred as well as any reinnervation by surviving motor neurons would be potential confounds. Instead, we used the soleus muscle from untreated B6.SOD1 mice for several reasons. Normally soleus is one of the most active muscles in the hindlimb (Hennig and Lomo, 1985), and does not contain fast motor units of the type that become denervated first in SOD1 mice (Frey et al., 2000; Hegedus et al., 2007; Hegedus et al., 2008; Pun et al., 2006). The B6.SOD1 soleus muscle is also likely to be naturally overloaded because of loss of innervation in close synergists such as the MG, LG and plantaris muscles which have lost 40–60% of their innervation by 100 days (Figure 1–2, (Carrasco et al., 2010)). Finally, soleus is comparably well innervated at 100 days, with an average of greater than 80% complete NMJ innervation (N = 3, Figure 3). The fact that some partially and completely denervated endplates are present, however, demonstrates that motor terminal degeneration is present in soleus muscles and has commenced by 100 days.

Endplate currents at soleus NMJs were first recorded with glucose present in the bathing fluid. Under these conditions, almost all measures of function at B6.SOD1 soleus NMJs were similar to wildtype. As shown in Table 1, average mEPC and EPC amplitudes and quantal content were all similar between wildtype and B6.SOD1 mice and did not differ significantly ($p > 0.05$, Tukey's HSD). Although mEPC frequency was higher on average in B6.SOD1 mice, the difference was not significant ($p > 0.05$, Tukey's HSD). More limited sampling showed that the rate of EPC amplitude depression during high frequency activation (50 Hz) was similar between wildtype and B6.SOD1 mice (Figure 4). This indicates that soleus motor terminals in B6.SOD1 mice do not show abnormal EPC depression during high frequency activation. These results show that synaptic transmission at B6.SOD1 soleus NMJs is similar to wildtype at 100 days when examined in glucose bathing media. This result is consistent with the presence of a large fraction of completely innervated NMJs also observed at 100 days (Figure 3). Since motor terminal degeneration had commenced in the studied soleus muscles, these data also suggest that significant preliminary synaptic dysfunction does not exist prior to motor terminal degeneration.

Mitochondrial dysfunction at B6.SOD1 soleus motor terminals

An increased susceptibility to reperfusion injury following ischemia has been demonstrated in B6.SOD1 motor terminals, but the effect was only observed in fast muscles as early as 31 days and not in soleus motor terminals as late as 100 days (David et al., 2007; Nguyen et al., 2011). We thus considered the possibility that despite any increased activity they may experience due to degenerative changes in synergist muscles, soleus motor terminals retain normal synaptic function in part because they possess intact mitochondria. In order to test this possibility, we sought to determine whether the relatively normal levels of function at soleus B6.SOD1 motor terminals found in glucose media (Figure 4) can be sustained when glycolysis is inhibited and ATP synthesis confined to mitochondria. Glycolysis can be inhibited by withdrawing glucose from the bathing media but the end product of glycolysis, pyruvate, must be replaced exogenously to enable continued mitochondrial respiration. Previous studies have shown that when this procedure is performed, synaptic transmission in a variety of preparations from normal tissue is maintained (Alvarez et al., 2003; Izumi et al., 1997; Izumi et al., 1994; Kauppinen and Nicholls, 1986a; Wang et al., 2003; Ying et al., 2002). In order to accomplish this test, in each soleus muscle examined, pyruvate was substituted for glucose in the bathing fluid, and additional sampling of NMJs was

performed. It is important to note that glucose and pyruvate (via glycolysis) are both present under normal conditions and that only glucose is absent under pyruvate-only conditions.

As shown in Figure 5A, inhibiting glycolysis produced few changes in the average values of properties of wildtype soleus neuromuscular transmission, and the changes that did occur were not significant. This result is consistent with other studies showing the pyruvate supports function at normal synapses (Alvarez et al., 2003; Izumi et al., 1997; Izumi et al., 1994; Wang et al., 2003; Ying et al., 2002). By contrast, at B6.SOD1 soleus NMJs, EPC failures in response to low frequency nerve stimulation (1 Hz) appeared in 2/5 preparations during electrical stimulation of motor axons. In one animal, 8/14 endplates examined after pyruvate substitution showed complete failure of EPC occurrence. In another 4/15 showed complete failure. Failures such as these were not observed after glycolysis inhibition and pyruvate substitution in all 5 wildtype soleus muscles or in any B6.SOD1 soleus muscles when bathed in glucose. Despite the appearance of these failures at some NMJs, no significant changes occurred after pyruvate substitution in mean mEPC amplitude, mean EPC amplitude, quantal content or high frequency (50 Hz) EPC depression at B6.SOD1 NMJs where motor terminals continued to release ACh in response to nerve electrical stimulation (Figure 5A). In B6.SOD1 soleus muscles tested, however, a large and significant increase in the frequency of spontaneous mEPCs was observed. While wildtype mean mEPC frequency remained at about 1 per sec after the pyruvate switch, average mEPC frequency in B6.SOD1 soleus muscles significantly increased to about 4.4 per sec, an approximately 4-fold increase over the average frequency observed in glucose (Figure 5A, $p < 0.05$, Tukey's HSD). Increases of mEPC frequency were observed in all 5 B6.SOD1 soleus muscles tested (Figure 5B). We did not sample mEPC frequency at individual NMJs both before and after the switch to pyruvate to determine the time course of mEPC frequency increase after glycolysis inhibition. However, mEPC frequency data obtained at various times after the switch to pyruvate in both wildtype and B6.SOD1 muscles did not reveal any obvious trend for mEPC frequency to increase with time after the switch (Figure 5C). This suggests that the increase of mEPC frequency at B6.SOD1 NMJs occurs soon after the inhibition of glycolysis. Evidence that average mEPC amplitude remained unchanged after pyruvate substitution indicates that factors such as endplate ACh receptor density and kinetics as well as quantal size remained unaffected. This suggests that the effects of pyruvate substitution were confined to the nerve terminal and not the result of alterations located postsynaptically.

Despite apparently normal performance in glucose bathing media, these results demonstrate that B6.SOD1 soleus motor terminals do not compensate for inhibition of glycolysis to the extent that wildtype motor terminals can compensate. This suggests that a dependence on glycolysis exists in B6.SOD1 soleus motor terminals that does not exist in wildtype motor terminals and indicates the presence of mitochondrial dysfunction at these terminals.

Mitochondrial dysfunction at HCSMA motor terminals

Because overload by synergist denervation accelerated motor terminal degenerative changes in muscles of HCSMA homozygotes (Carrasco et al., 2004), we were interested in determining whether evidence for mitochondrial dysfunction could be detected in HCSMA motor terminals. To determine this, the effects of glycolysis inhibition were tested on NMJs from 2 HCSMA homozygotes and compared with results obtained from one normal, control dog, all aged about 4–5 months. Recordings were obtained from fibers in biopsies of MG muscles, as described previously (Rich et al., 2002a; Rich et al., 2002b). The HCSMA homozygotes used in this study were approximately the age of homozygotes studied previously after 1 month of synergist denervation of the MG muscle (Carrasco et al., 2004). At these ages, motor units in the HCSMA homozygote MG normally exhibit significant failure manifested as an inability to sustain force output during repetitive activation (Pinter et al., 1995). At the same age, neuromuscular transmission in the homozygote MG differs

significantly from normal when examined in glucose bathing media and shows defects including a pronounced decrease in quantal content due to decreased nerve-evoked release of ACh (Rich et al., 2002a; Rich et al., 2002b). EPC amplitude at many NMJs is highly variable, and complete EPC failure in response to low frequency (1 Hz) nerve stimulation is common. Thus, synaptic dysfunction in HCSMA MG muscles used here is more advanced than in the B6.SOD1 soleus muscle studied above. At the level of the whole animal, the HCSMA homozygotes used here exhibited more movement disability and more disease progression than is observed in the B6.SOD1 mice of the ages used in this study.

Figure 6 shows that no significant changes in neuromuscular transmission were observed following elimination of glucose and substitution of pyruvate at normal dog NMJs, similar to observations made in wildtype mice. However, following inhibition of glycolysis, changes occurred in neuromuscular transmission that resembled those found in B6.SOD1 mice. Specifically, average mEPC frequency increased about 2.6-fold and the average rate of 1 Hz EPC failure increased almost 3.4-fold, both changes being significant ($p < 0.05$, Tukey's HSD). mEPC amplitudes remained unchanged at homozygote NMJs after pyruvate substitution indicating that mEPC frequency changes and EPC failures were presynaptic phenomena. At NMJs where ACh release continued after pyruvate substitution, mean EPC amplitude declined slightly so that quantal contents decreased but not significantly. Insufficient data were collected to enable determining effects on high frequency (50 Hz) EPC depression. These results demonstrate the presence of mitochondrial dysfunction at HCSMA motor terminals as well as a dependence on glycolysis which resembles that observed at motor terminals of B6.SOD1 mice.

Discussion

This study was designed to determine whether activity contributes to motor terminal degeneration in B6.SOD1 mice. The idea that activity might contribute to motor terminal degeneration was based in part on evidence for mitochondrial dysfunction in B6.SOD1 mice, particularly at the motor terminal (David et al., 2007; Nguyen et al., 2011). The role of activity is envisioned as promoting degenerative changes by increasing demand for metabolic support from mitochondria that are made progressively less capable of providing support by the direct or indirect actions of mutated protein. Previously, direct evidence that activity accelerated motor terminal degeneration in HCSMA was obtained after overloading hindlimb muscles by denervation of all close synergists for a 1 month period (Carrasco et al., 2004). Evidence from this study now shows the presence of mitochondrial dysfunction at HCSMA motor terminals (Figure 6). In B6.SOD1 mice, however, overload for a 2 month period produced no detectable effects on the degeneration of B6.SOD1 plantaris motor terminals.

An important question is whether the design of this study provided sufficient conditions to detect an activity effect in B6.SOD1 mice. Overload treatment began well before significant denervation appears in the plantaris muscle, so the increased activity caused by overload was present before motor terminal degeneration initiated. Moreover, overloaded plantaris muscles had increased weight, consistent with muscle fiber hypertrophy secondary to increased use. Plantaris muscle contains about 40% type IIb muscle fibers (Burkholder et al., 1994), and these fibers are known to lose innervation before other types in SOD1 mice (Frey et al., 2000; Hegedus et al., 2007; Hegedus et al., 2008; Pun et al., 2006). It is thus possible that an effect to accelerate degeneration of motor terminals supplying these fibers types may have been missed by examining results later in the disease course when much or all IIb innervation may normally be lost. If increased activity did act to accelerate denervation of these fiber types, then it would be expected that TTX blockade of motor terminal activity should slow the rate of degeneration among plantaris motor terminals. The results of our

TTX paralysis experiments, however, showed that elimination of motor terminal activity for 1 month did not slow degeneration of any plantaris motor terminals even though TTX treatment began at about the same time as motor terminal degeneration begins in the plantaris muscle. It cannot be excluded that commencing TTX treatment at an earlier age or more prolonged TTX treatment may have slowed motor terminal degeneration. However, this possibility seems unlikely since no indication of such effects could be detected after complete motor terminal inactivity during a month interval in which we estimate that 25–50% of plantaris motor terminals normally degenerate in B6.SOD1 mice (Figures 1–2). We also found that motor terminals in untreated B6.SOD1 soleus muscles showed relatively normal function in glucose bathing media even though the tested soleus muscles were likely to experience increased activity during the natural disease course as a result of loss of innervation in synergist muscles. Overall, these data provide no support for a role of activity in mediating or accelerating motor terminal degeneration in B6.SOD1 mice.

Increased activity caused by overload has recently been reported to prevent or inhibit disease-related loss of motor unit numbers in B6.SOD1 mice (Gordon et al., 2010). Comparison of this finding with the present results is difficult because we did not examine motor unit numbers in this study, and there are other differences in design which may be significant. However, assuming that the total number of plantaris muscle fibers did not differ between sides after overload in the present study, any increase of motor unit number in overloaded plantaris muscles would have little functional consequence since overload did not affect the total number of innervated muscle fibers.

Possible compensatory mechanisms

One implication of these results is that the mechanisms underlying motor terminal degeneration proceed independently of activity in B6.SOD1 mice. Another implication is that the metabolic capacity of the tested motor terminals is sufficient to handle the levels of increased activity that the animal imposed naturally and that we imposed experimentally, despite evidence for mitochondrial dysfunction in B6.SOD1 mice. Possible explanations include that mitochondrial damage in B6.SOD1 motor terminals is not sufficient to interrupt metabolic support for activity and maintenance of resting conditions or that damage provokes mitochondrial cell death functions first and this process leads to degeneration.

Another possibility for explaining how sufficient metabolic capacity is maintained to meet demands of activity and resting conditions is that other mechanisms compensate for loss of mitochondrial metabolic capacity. Support for this possibility was provided by the results of our experiments in which glycolysis was inhibited while recording NMJ synaptic properties in B6.SOD1 soleus muscle fibers. Since pyruvate is the end product of glycolysis and is oxidized by mitochondria, ATP production can be confined to oxidative phosphorylation pathways in mitochondria by substituting pyruvate for glucose in bathing fluids. Consistent with previous studies (Kauppinen and Nicholls, 1986b), wildtype soleus and normal dog motor terminals showed no change in function when this substrate switch was made, reflecting the presence of fully functional mitochondria. However, a large increase in the average frequency of mEPCs and blocking of evoked release in some B6.SOD1 preparations was observed after glycolysis inhibition and pyruvate substitution in B6.SOD1 soleus motor terminals (Figure 5). Qualitatively similar changes were observed at HCSMA homozygote motor terminals (Figure 6), but upon a background of greater synaptic dysfunction when examined in glucose.

The types of synaptic function changes observed after the glucose-pyruvate switch are generally considered to be located presynaptically. Supporting this is the lack of any change of the amplitude of mEPCs recorded in B6.SOD1 and HSCMA fibers after the pyruvate switch (Figures 5 and 6). Insight into possible mechanisms can be gained by consideration

of experimental manipulations that provoke the same changes at normal motor terminals. There are a variety of experimental manipulations that increase mEPC frequency including increases of Ca2+ and osmotic pressure in bathing fluid (Hubbard, 1961; Liley, 1956; Van der Kloot and Molgo, 1994). However, increases of extracellular K+ concentration are known to increase the frequency of mEPCs at motor terminals as well as provoke blocking of evoked release at motor terminals (Rich et al., 2002b). Underlying the effects of increased extracellular K+ concentration is a reduced plasma membrane K+ gradient and depolarization of the terminal membrane which increases Na+ channel inactivation and Ca2+ entry which, respectively, produce blockade of action potentials and increased mEPC frequency. In support of this possibility, when otherwise normal synaptosomes are deprived of glucose, mitochondrial respiration and oxidative phosphorylation fail for lack of substrate when pyruvate is not supplied and a decreased plasma membrane K+ gradient occurs as a result (Bradford et al., 1978). Thus, a reasonable theory to account for our observations is that after glycolysis inhibition and the switch to pyruvate-containing bathing media, the motor terminal membrane depolarizes. The simplest explanation for these effects is that mitochondria in both SOD1 soleus and HCSMA motor terminals are unable to completely support baseline metabolic needs after glycolysis is inhibited even though pyruvate is freely available as a substrate for respiration and oxidative phophorylation. Moreover, if dysfunctional mitochondria feature reversed operation of the ATP synthase, sequestered Ca2+ could be released into the terminal as mitochondria depolarize during depletion of residual ATP from glycolysis (Nicholls et al., 2000).

An additional consideration is the possibility that exogenous pyruvate may have increased reactive oxygen species (ROS) in SOD1 motor terminals. Exogenous pyruvate hyperpolarizes the mitochondrial resting potential in synaptosomes (Choi et al., 2009; Kauppinen and Nicholls, 1986b), and we have seen evidence of this effect in normal mouse motor terminals using vital dyes to monitor mitochondrial resting potential (unpublished). The hyperpolarizing effect is thought to arise because of increased respiration due to increased availability of pyruvate, the supply of which is normally limited by glycolysis (Brand and Nicholls, 2011; Kauppinen and Nicholls, 1986b). Evidence shows that hyperpolarization of mitochondria increases ROS production (Boveris et al., 1972; Korshunov et al., 1997), and other studies have shown that mitochondria isolated from brain and spinal cord of SOD1 rats exhibit increased ROS production (Panov et al., 2011). It is thus possible that pyruvate may have acted to aggravate preexisting mitochondrial dysfunction or other motor terminal damage by an indirect action to increase ROS production.

The extent to which glycolysis may be able to compensate for dysfunctional motor terminal mitochondria is unknown, but other studies indicate that in synaptosomes, glycolysis can upregulate 10-fold (Kauppinen and Nicholls, 1986b). It is conceivable that degenerative changes may commence in motor terminals when glycolytic compensation fails to adapt sufficiently to progressive loss of mitochondrial function. At this point, very limited amounts of increased metabolic demand could initiate degenerative changes. Differences in the capacity of this compensation may help explain why HCSMA motor terminals are susceptible to increased activity while B6.SOD1 motor terminals are not, as well as the earlier degeneration of motor terminals innervating fast muscle fibers in B6.SOD1 mice. Although NMJ synaptic function in HCSMA dogs and B6.SOD1 mice shows a similar response to glycolysis inhibition, it is important to note other important differences between these models and that they should be compared with some caution. Most important among these is a difference in underlying genetic mechanisms. Although the identity of the defective gene in HCSMA remains unknown, it is known that the SOD1 gene is not mutated in HCSMA (Green et al., 2002). As noted earlier, the temporal pattern of motor unit type involvement also differs with slow units showing dysfunction in HCSMA first while fast

units are lost first in the SOD1 mouse. In terms of the emergence of observable symptoms, HCSMA homozygotes show a relatively early, juvenile onset and a more rapid progression rate than the SOD1 mouse. In addition, HCSMA motor terminals show considerable synaptic dysfunction prior to degeneration (Fischer et al., 2004; Rich et al., 2002a; Rich et al., 2002b) whereas surviving motor terminals in the B6.SOD1 soleus muscle appear to exhibit very little dysfunction (Table 1) even though motor terminal degeneration is present in the muscle (Figure 3). Given the probable existence of other differences, it thus seems best to characterize similarities in the response to glycolytic inhibition as an indication that different disease mechanisms eventually converge to produce the common factor of mitochondrial dysfunction and consequent glycolytic compensation.

More generally, limits on the ability of glycolysis to compensate for mitochondrial dysfunction may be a factor that increases motor terminal vulnerability and perhaps other synapses in the presence of diminished mitochondrial metabolic capacity. The range of glycolytic compensation for mitochondrial dysfunction may be more restricted in motor terminals than in cell bodies where transcriptional mechanisms needed for extensive upregulation of glycolytic pathways are more readily accessible. Further focus on these compensatory mechanisms could provide new therapeutic targets.

Acknowledgments

This work was supported by NIH grant NS31621 (MJP).

References

Alvarez G, Ramos M, Ruiz F, Satrustegui J, Bogonez E. Pyruvate protection against beta-amyloid-induced neuronal death: role of mitochondrial redox state. J Neurosci Res. 2003; 73:260–9. [PubMed: 12836169]

Babcock DF, Hille B. Mitochondrial oversight of cellular Ca2+ signaling. Curr Opin Neurobiol. 1998; 8:398–404. [PubMed: 9687353]

Balice-Gordon RJ, Smith DB, Goldman J, Cork LC, Shirley A, Cope TC, et al. Functional motor unit failure precedes neuromuscular degeneration in canine motor neuron disease. Ann Neurol. 2000; 47:596–605. [PubMed: 10805330]

Boveris A, Oshino N, Chance B. The cellular production of hydrogen peroxide. Biochem J. 1972; 128:617–30. [PubMed: 4404507]

Bradford HF, Ward HK, Thomas AJ. Glutamine--a major substrate for nerve endings. J Neurochem. 1978; 30:1453–9. [PubMed: 670985]

Brand MD, Nicholls DG. Assessing mitochondrial dysfunction in cells. Biochem J. 2011; 435:297–312. [PubMed: 21726199]

Burkholder TJ, Fingado B, Baron S, Lieber RL. Relationship between muscle fiber types and sizes and muscle architectural properties in the mouse hindlimb. J Morphol. 1994; 221:177–90. [PubMed: 7932768]

Carrasco DI, Bichler EK, Seburn KL, Pinter MJ. Nerve terminal degeneration is independent of muscle fiber genotype in SOD1 mice. PLoS One. 2010; 5:e9802. [PubMed: 20339550]

Carrasco DI, Rich MM, Wang Q, Cope TC, Pinter MJ. Activity-driven synaptic and axonal degeneration in canine motor neuron disease. J Neurophysiol. 2004; 92:1175–81. [PubMed: 15028742]

Carreras I, Yuruker S, Aytan N, Hossain L, Choi JK, Jenkins BG, et al. Moderate exercise delays the motor performance decline in a transgenic model of ALS. Brain Res. 2010; 1313:192–201. [PubMed: 19968977]

Choi SW, Gerencser AA, Nicholls DG. Bioenergetic analysis of isolated cerebrocortical nerve terminals on a microgram scale: spare respiratory capacity and stochastic mitochondrial failure. J Neurochem. 2009; 109:1179–91. [PubMed: 19519782]

Damiano M, Starkov AA, Petri S, Kipiani K, Kiaei M, Mattiazzi M, et al. Neural mitochondrial Ca2+ capacity impairment precedes the onset of motor symptoms in G93A Cu/Zn-superoxide dismutase mutant mice. J Neurochem. 2006; 96:1349–61. [PubMed: 16478527]

David G, Nguyen K, Barrett EF. Early vulnerability to ischemia/reperfusion injury in motor terminals innervating fast muscles of SOD1-G93A mice. Exp Neurol. 2007; 204:411–20. [PubMed: 17292357]

Fischer LR, Culver DG, Tennant P, Davis AA, Wang M, Castellano-Sanchez A, et al. Amyotrophic lateral sclerosis is a distal axonopathy: evidence in mice and man. Exp Neurol. 2004; 185:232–40. [PubMed: 14736504]

Frey D, Schneider C, Xu L, Borg J, Spooren W, Caroni P. Early and selective loss of neuromuscular synapse subtypes with low sprouting competence in motorneuron diseases. J Neurosci. 2000; 20:2534–2542. [PubMed: 10729333]

Garcia-Chacon LE, Nguyen KT, David G, Barrett EF. Extrusion of Ca2+ from mouse motor terminal mitochondria via a Na+-Ca2+ exchanger increases post-tetanic evoked release. J Physiol. 2006; 574:663–75. [PubMed: 16613870]

Gardiner P, Michel R, Browman C, Noble E. Increased EMG of rat plantaris during locomotion following surgical removal of its synergists. Brain Res. 1986; 380:114–21. [PubMed: 3756465]

Gordon T, Tyreman N, Li S, Putman CT, Hegedus J. Functional over-load saves motor units in the SOD1-G93A transgenic mouse model of amyotrophic lateral sclerosis. Neurobiol Dis. 2010; 37:412–22. [PubMed: 19879358]

Green SL, Tolwani RJ, Varma S, Quignon P, Galibert F, Cork LC. Structure, chromosomal location, and analysis of the canine Cu/Zn superoxide dismutase (SOD1) gene. J Hered. 2002; 93:119–24. [PubMed: 12140271]

Gurney ME, Pu H, Chiu AY, Dal Canto MC, Polchow CY, Alexander DD, et al. Motor neuron degeneration in mice that express a human Cu, Zn superoxide dismutase mutation. Science. 1994; 264:1772–5. [PubMed: 8209258]

Hegedus J, Putman CT, Gordon T. Time course of preferential motor unit loss in the SOD1 G93A mouse model of amyotrophic lateral sclerosis. Neurobiol Dis. 2007; 28:154–64. [PubMed: 17766128]

Hegedus J, Putman CT, Tyreman N, Gordon T. Preferential motor unit loss in the SOD1 G93A transgenic mouse model of amyotrophic lateral sclerosis. J Physiol. 2008; 586:3337–51. [PubMed: 18467368]

Hennig R, Lomo T. Firing patterns of motor units in normal rats. Nature. 1985; 314:164–166. [PubMed: 3974720]

Hubbard JI. The effect of calcium and magnesium on the spontaneous release of transmitter from mammalian motor nerve endings. J Physiol. 1961; 159:507–17. [PubMed: 14449608]

Izumi Y, Benz AM, Katsuki H, Zorumski CF. Endogenous monocarboxylates sustain hippocampal synaptic function and morphological integrity during energy deprivation. J Neurosci. 1997; 17:9448–57. [PubMed: 9391000]

Izumi Y, Benz AM, Zorumski CF, Olney JW. Effects of lactate and pyruvate on glucose deprivation in rat hippocampal slices. Neuroreport. 1994; 5:617–20. [PubMed: 8025256]

Kauppinen RA, Nicholls DG. Pyruvate utilization by synaptosomes is independent of calcium. FEBS Lett. 1986a; 199:222–6. [PubMed: 3084295]

Kauppinen RA, Nicholls DG. Synaptosomal bioenergetics. The role of glycolysis, pyruvate oxidation and responses to hypoglycaemia. Eur J Biochem. 1986b; 158:159–65. [PubMed: 2874024]

Kirkinezos IG, Hernandez D, Bradley WG, Moraes CT. Regular exercise is beneficial to a mouse model of amyotrophic lateral sclerosis. Ann Neurol. 2003; 53:804–7. [PubMed: 12783429]

Korshunov SS, Skulachev VP, Starkov AA. High protonic potential actuates a mechanism of production of reactive oxygen species in mitochondria. FEBS Lett. 1997; 416:15–8. [PubMed: 9369223]

Liley AW. The effects of presynaptic polarization on the spontaneous activity at the mammalian neuromuscular junction. J Physiol. 1956; 134:427–43. [PubMed: 13398923]

Mahoney DJ, Rodriguez C, Devries M, Yasuda N, Tarnopolsky MA. Effects of high-intensity endurance exercise training in the G93A mouse model of amyotrophic lateral sclerosis. Muscle Nerve. 2004; 29:656–62. [PubMed: 15116368]

Nguyen KT, Barrett JN, Garcia-Chacon L, David G, Barrett EF. Repetitive nerve stimulation transiently opens the mitochondrial permeability transition pore in motor nerve terminals of symptomatic mutant SOD1 mice. Neurobiol Dis. 2011; 42:381–90. [PubMed: 21310237]

Nicholls D, Bernardi P, Brand M, Halestrap A, Lemasters J, Reynolds I. Apoptosis and the laws of thermodynamics. Nat Cell Biol. 2000; 2:E172–3. [PubMed: 11025673]

Nicholls, DG.; Fergusen, SJ. Bioenergetics. Vol. 3. Academic Press; London: 2002.

Panov A, Kubalik N, Zinchenko N, Hemendinger R, Dikalov S, Bonkovsky HL. Respiration and ROS production in brain and spinal cord mitochondria of transgenic rats with mutant G93a Cu/Zn-superoxide dismutase gene. Neurobiol Dis. 2011; 44:53–62. [PubMed: 21745570]

Panov, A.; Steuerwald, N.; Vavilin, V.; Dambinova, S.; Bonkovsky, HL. Role of neuronal mitochondrial metabolic phenotype in pathogenesis of ALS. In: Maurer, MH., editor. Amyotrophic Lateral Sklerosis. Intech Open Access Publisher; 2012. p. 225-248.

Pearson KG, Fouad K, Misiaszek JE. Adaptive changes in motor activity associated with functional recovery following muscle denervation in walking cats. J Neurophysiol. 1999; 82:370–81. [PubMed: 10400965]

Pedrini S, Sau D, Guareschi S, Bogush M, Brown RH Jr, Naniche N, et al. ALS-linked mutant SOD1 damages mitochondria by promoting conformational changes in Bcl-2. Hum Mol Genet. 2010; 19:2974–86. [PubMed: 20460269]

Pinter, MJ.; Cope, T.; Cork, LC.; Green, SL.; Rich, MM. Canine motor neuron disease: A view from the motor unit. In: Cope, TC., editor. Motor Neurobiology of the Spinal Cord. CRC Press; Boca Raton, FL: 2001. p. 231-250.

Pinter MJ, Waldeck RF, Wallace N, Cork LC. Motor Unit Behavior in Canine Motor Neuron Disease. J Neurosci. 1995; 15:3447–3457. [PubMed: 7751923]

Pun S, Santos AF, Saxena S, Xu L, Caroni P. Selective vulnerability and pruning of phasic motoneuron axons in motoneuron disease alleviated by CNTF. Nat Neurosci. 2006; 9:408–19. [PubMed: 16474388]

Rich MM, Waldeck RF, Cork LC, Balice-Gordon RJ, Fyffe REW, Wang X, et al. Reduced endplate currents provoke motor unit dysfunction while axonal functional properties mature normally in canine motor neuron disease. J Neurophysiol. 2002a; 88:3293–3304. [PubMed: 12466447]

Rich MM, Wang X, Cope TC, Pinter MJ. Reduced quantal content with normal synaptic release time course and depression characterize failure of neuromuscular transmission in canine motor neuron disease. J Neurophysoiol. 2002b; 88:3305–3314.

Santa-Cruz, LD.; Ramírez-Jarquín, UN.; Tapia, R. Role of Mitochondrial Dysfunction in Motor Neuron Degeneration in ALS. In: Maurer, MH., editor. Amyotrophic Lateral Sklerosis. Intech Open Access Publisher; 2012. p. 197-224.

Van der Kloot W, Molgo J. Quantal acetylcholine release at the vertebrate neuromuscular junction. Physiol Rev. 1994; 74:899–992. [PubMed: 7938228]

Veldink JH, Bar PR, Joosten EA, Otten M, Wokke JH, van den Berg LH. Sexual differences in onset of disease and response to exercise in a transgenic model of ALS. Neuromuscul Disord. 2003; 13:737–43. [PubMed: 14561497]

Wang XQ, Xiao AY, Sheline C, Hyrc K, Yang A, Goldberg MP, et al. Apoptotic insults impair Na+, K+-ATPase activity as a mechanism of neuronal death mediated by concurrent ATP deficiency and oxidant stress. J Cell Sci. 2003; 116:2099–110. [PubMed: 12679386]

Wooley CM, Sher RB, Kale A, Frankel WN, Cox GA, Seburn KL. Gait analysis detects early changes in transgenic SOD1(G93A) mice. Muscle Nerve. 2005; 32:43–50. [PubMed: 15880561]

Ying W, Chen Y, Alano CC, Swanson RA. Tricarboxylic acid cycle substrates prevent PARP-mediated death of neurons and astrocytes. J Cereb Blood Flow Metab. 2002; 22:774–9. [PubMed: 12142562]

Yoshikami D, Okun LM. Staining of living presynaptic nerve terminals with selective fluorescent dyes. Nature. 1984; 310:53–6. [PubMed: 6610832]

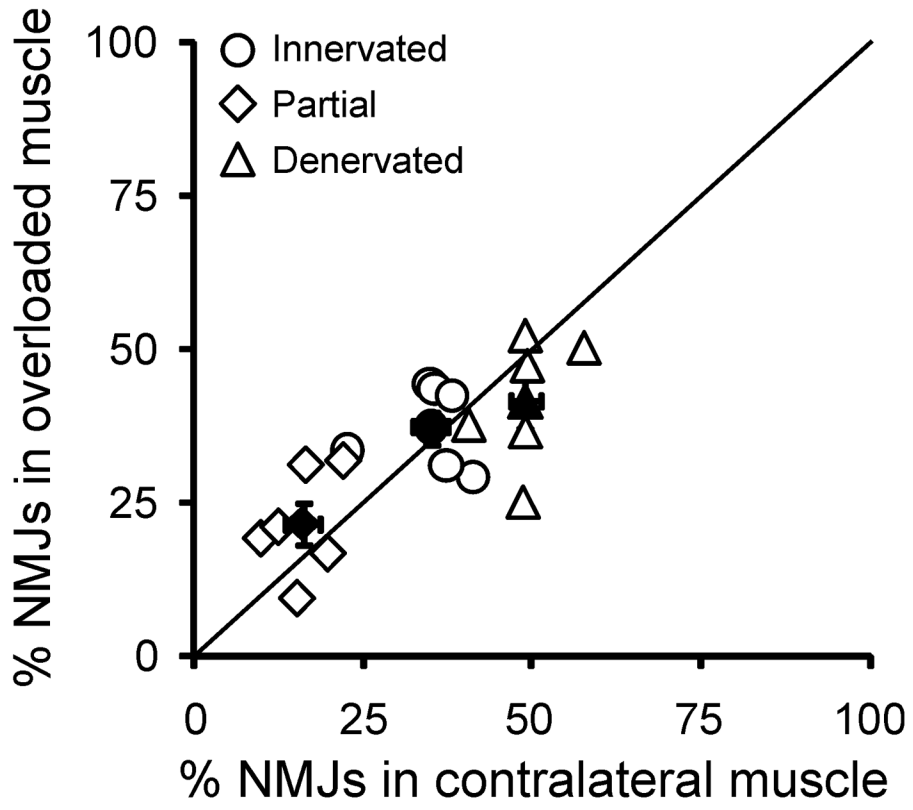

Figure 1.

Overload of plantaris muscle in B6.SOD1 mice by synergist denervation does not affect motor terminal degeneration. Scatter plot shows percentages of innervated, partially innervated and denervated endplates (open symbols, see inset) in B6.SOD1 plantaris muscles 2 months following denervation of all close synergists plotted against percentages obtained from contralateral, untreated plantaris muscles. Filled symbols indicate mean values for each endplate category (N = 4 animals). Endplate category percentages from overloaded plantaris muscles did not differ significantly from contralateral percentages. Straight line indicates unity slope.

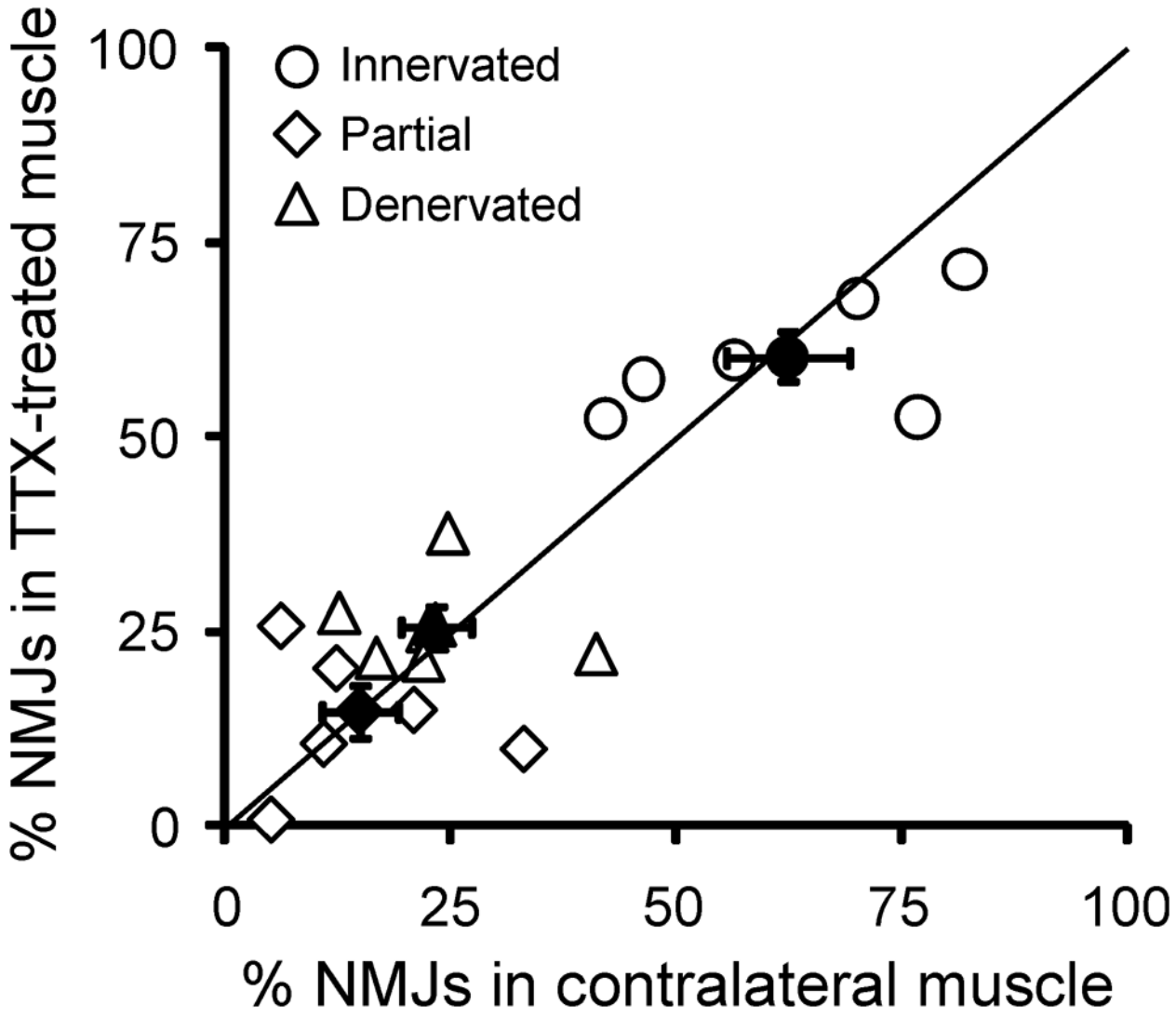

Figure 2.

Paralysis of plantaris muscle in B6.SOD1 mice by blockade of sciatic nerve conduction does not affect motor terminal degeneration. Scatter plot shows percentages of innervated, partially innervated and denervated endplates in B6.SOD1 plantaris muscles (open symbols) 1 month following placement of a TTX cuff around the sciatic nerve plotted against percentages obtained from contralateral, untreated plantaris muscles. Filled symbols indicate mean values for each endplate category (N = 4 animals). Endplate category percentages from overloaded plantaris muscles did not differ significantly from contralateral percentages. Straight line indicates unity slope.

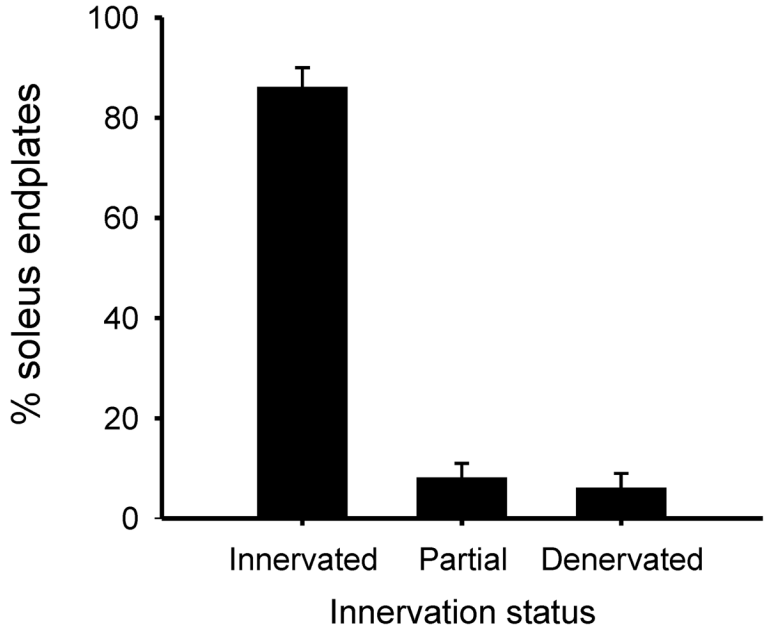

Figure 3.
Innervation status of B6.SOD1 soleus. Bar chart shows innervation status of endplates in B6.SOD1 soleus muscles from mice aged about 100 days (N = 3). At this stage of disease progression, the soleus muscle remains comparably well innervated.

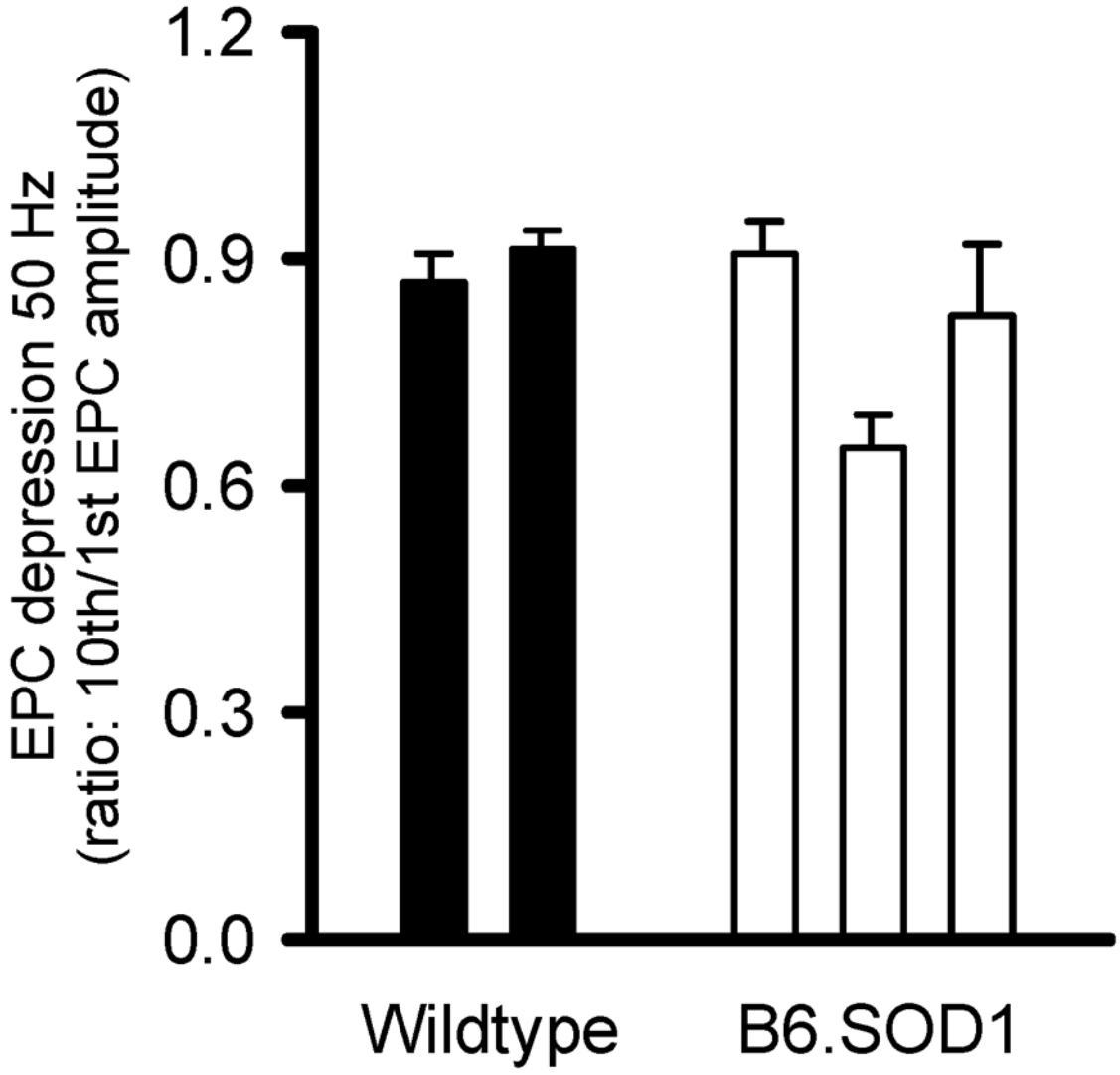

Figure 4.

EPC depression during repetitive, high frequency activation at B6.SOD1 and wildtype soleus NMJs. Bar charts show data from individual wildtype and B6.SOD1 mice and specify the average ratio between amplitudes of the 10th and first EPCs in a train of 10 EPCs activated at 50 Hz. Data were obtained with glucose in the bathing fluid.

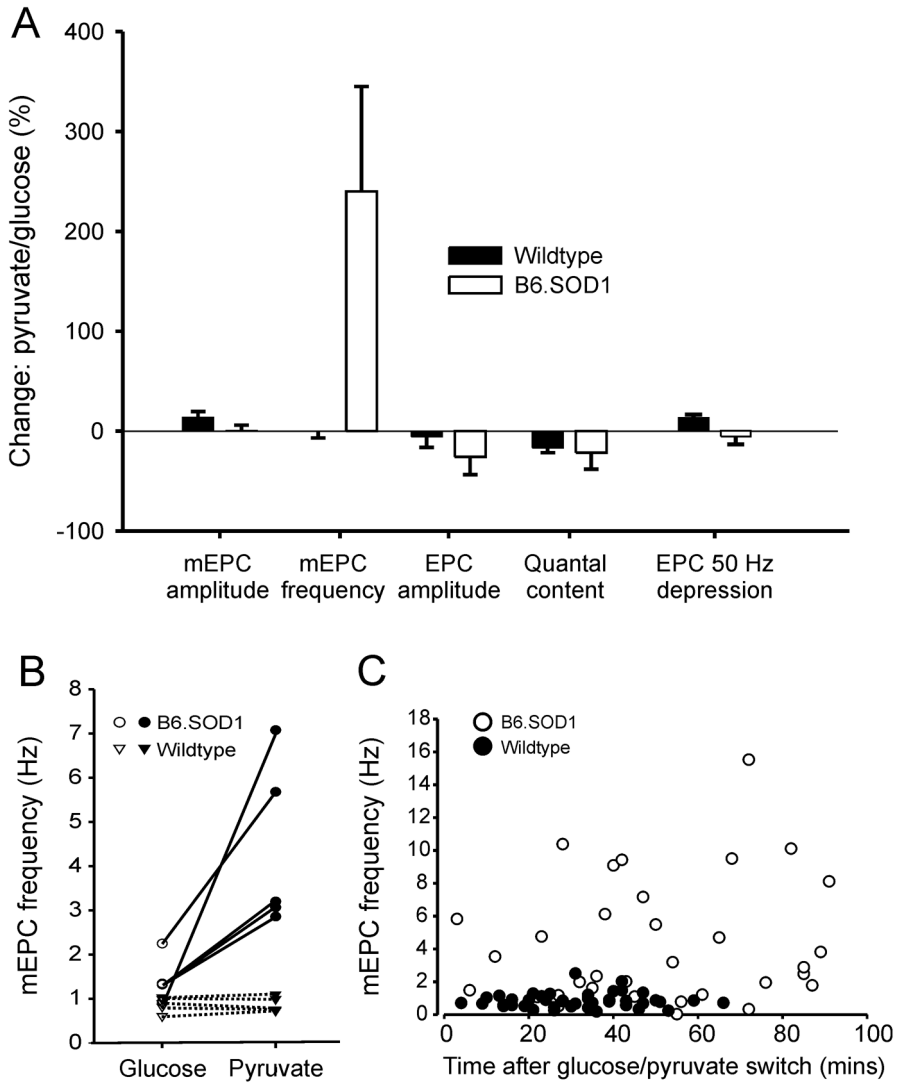

Figure 5.

Wildtype and B6.SOD1 soleus NMJ synaptic transmission properties after elimination of glycolysis. A. Bar charts show the average of the means for each property obtained after elimination of glucose and substitution of exogenous pyruvate to the bathing media expressed as a percentage of the mean values obtained in glucose. Data are based on recordings from a minimum of 7 muscle fibers obtained in glucose media and after elimination of glucose and addition of exogenous pyruvate in each soleus muscle from 5 wildtype and B6.SOD1 mice. The increase of mEPC frequency in B6.SOD1 soleus after the pyruvate switch was statistically significant ($p < 0.01$). B. Plot shows mean mEPC frequency in glucose and after pyruvate switch for individual B6.SOD1 and wildtype soleus muscles. C. Plot shows mean mEPC frequency at individual wildtype and B6.SOD1 soleus NMJs measured at various times after eliminating glucose and substituting pyruvate in the bathing media. Note that NMJs were sampled at only one time point and that no clear trend is evident for mEPC frequency to increase or decrease with time at either wildtype or B6.SOD1 NMJs.

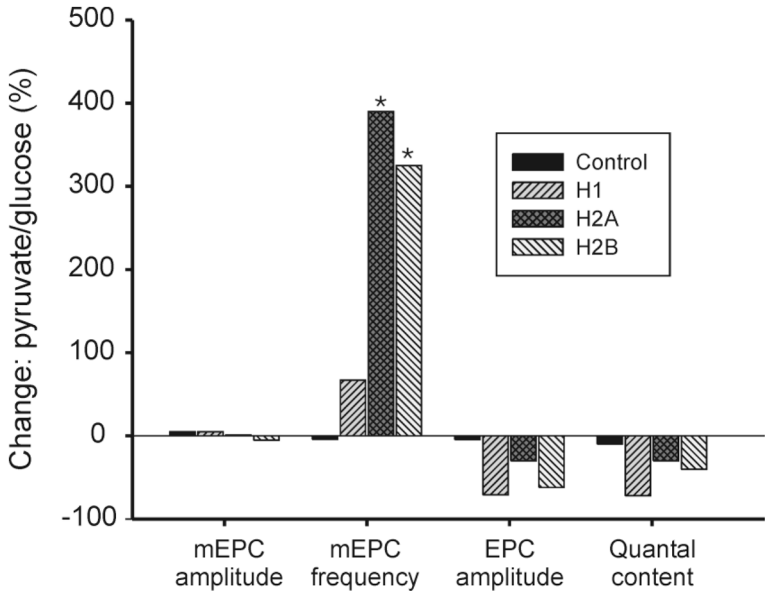

Figure 6.

Control and homozygote HCSMA MG NMJ synaptic transmission properties after elimination of glycolysis. Data are from one control animal and 2 homozygotes. One homozygote (H2) provided 2 biopsies from medial gastrocnemius (MG) muscles (see inset). Each bar shows results from a single MG muscle biopsy and represents the mean value for each property obtained after eliminating glucose and adding exogenous pyruvate to the bathing media expressed as a percentage of the mean value obtained with glucose in the bath media. Data are based on recordings from a minimum of 5 muscle fibers obtained in glucose media and after elimination of glucose and addition of exogenous pyruvate. Asterisks (*) indicate statistically significant ($p < 0.05$) change of mean value (t-test).

Table 1

B6.SOD1 and wildtype soleus NMJ synaptic properties recorded in glucose media

N = 5	mEPC amplitude (nA)	mEPC frequency (Hz)	EPC amplitude (nA)	Quantal content
Wildtype	1.7 ± 0.1	0.9 ± 0.1	88.4 ± 6.6	50.9 ± 2.1
B6.SOD1	1.4 ± 0.1	1.4 ± 0.2	70.0 ± 10.9	48.5 ± 3.7

Mean values are shown ± SEM